ACS Macro Letters

pubs.acs.org/macroletters
Letter

Charge Scaling in Classical Force Fields for Lithium Ions in Polymers

Dongyue Liang, Yuxi Chen, Chuting Deng, and Juan J. de Pablo*

Cite This: ACS Macro Lett. 2024, 13, 1258–1264
Read Online

ABSTRACT: Polymer electrolytes are of interest for applications in energy storage. Molecular simulations of ion transport in polymer electrolytes have been widely used to study the conductivity in these materials. Such simulations have generally relied on classical force fields. A peculiar feature of such force fields has been that in the particular case of lithium ions (Li^+), their charge must be scaled down by approximately 20% to achieve agreement with experimental measurements of ion diffusivity. In this work, we present first-principles calculations that serve to justify the charge-scaling factor and van der Waals interaction parameters for Li^+ diffusion in poly(ethylene glycol) (PEO) with bistriflimide ($TFSI^-$) counterions. Our results indicate that a scaling factor of 0.79 provides good agreement with DFT calculations over a relatively wide range of Li^+ concentrations and temperatures, consistent with past reports where that factor was adjusted by trial and error. We also show that such a scaling factor leads to diffusivities that are in quantitative agreement with experimental measurements.

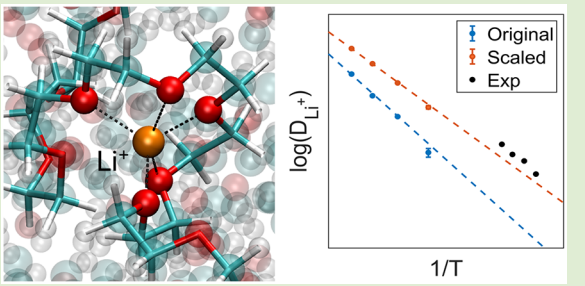

Polymer electrolytes represent an important class of solid-state electrolytes for applications in energy storage.[1−3] Over the past decade, various studies of polymer electrolytes have relied on molecular dynamics (MD) simulations with pairwise additive force fields to arrive at a detailed picture of molecular structure, mobility, and diffusion in such materials.[4−8]

Past studies of Li^+ transport in polymers with classical nonpolarizable force fields have recognized that Li^+ are overstabilized by water when their full charge of $+1e$ is assigned to them. This overly strong binding leads to properties that deviate from the experimental measurements. Several studies have addressed this issue by scaling down the Li^+ charge by a factor in the range from 0.7 to 0.8.[9−19] Such charge-scaled models have also been considered in other contexts of ionic solvation,[12,20−22] and for some cases, intuitive physical pictures have been advanced. Kann and Skinner,[20] for example, proposed a scaled-ionic-charge model for aqueous salt solutions and attributed the use of a scaling factor to the need for a phenomenological electronic continuum that compensates for the inability of nonpolarizable water models to reproduce experimental dielectric constants, as initially suggested by Leontyev and Stuchebrukhov.[23]

In the particular case of Li^+ transport in polymer melts, the scaling of ionic charge is significant enough to impact both the ion coordination and its dynamics.[9,10,13,24] In practice, past studies have arrived at numerical values of the scaling factor by a trial-and-error approach.[9] Several works have sought to determine the magnitude of the scaling factor by relying on quantum-mechanical calculations and have reported scaling factors in the range of 0.55−0.8.[10,11,18] One possible cause for this broad range could be the sensitivity of the electrostatic potential charge analysis[25] to the specific structures or environment of interest. The physical basis of the scaling has sometimes been interpreted through the concept of charge transfer.[11] Our preliminary Bader analysis[26] on a periodic simulation cell with a Li^+:EO ratio of 1:10 (here the Li^+:EO ratio stands for the ratio of number of Li^+ over number of PEO oxygen atoms in the system; see the Supporting Information for details of a Bader charge analysis), however, suggests that Li^+ carries $+0.9e$ on average, which is larger than the commonly applied charge-scaling factors. We thus assume that an optimum scaling factor might have to implicitly consider multiple effects including charge transfer, induced polarization, and the conditions of nonpolarizable force field parametrization.[16,21,24] Additionally, in the case of polymer electrolytes, the van der Waals parameters that are commonly used (which generally adopt a Lennard-Jones (LJ) form) are often not specifically developed for the case of ion transport in polymers. In simulations of proteins and biomolecules, it is commonly acknowledged that the use of "non-bonded fix" (known as NBFIX or CUFIX) parameters[27,28] improves bonded interactions and free energies, and the LJ parameters can be improved along such lines.

Received: May 31, 2024
Revised: August 20, 2024
Accepted: August 22, 2024

In this work, we focus on the Li^+−$TFSI^-$−PEO system (Figure 1), which can be viewed as a well-studied prototype for

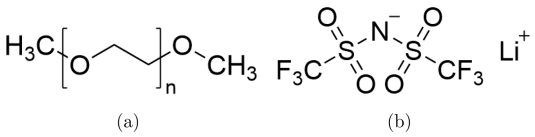

Figure 1. Structural formulas of PEO and Li^+−$TFSI^-$ ions.

polymer electrolytes. We start from the existing OPLS force field,[29−31] which is widely used for simulations of ionic liquids and polymer melts. That force field is then modified as follows: first, the charge on each of the atoms of the Li^+−$TFSI^-$ salt is scaled by a uniform factor. Second, we modify the LJ parameters between the Li−O types for Li^+−PEO and Li^+−$TFSI^-$ interactions. An alternative strategy, where the charges on both ions and polymers are scaled, has been proposed in previous works.[11,32] Here we note that in the case of ion-binding proteins, scaling the partial charges on both the ion and the protein was found necessary to capture the thermodynamics.[32] Because we want to preserve a description in terms of the original OPLS force field, which is used extensively to calculate the bulk properties of liquids from molecular parametrizations,[29] we chose not to pursue such a strategy in this work. In our case, the five new parameters required by the force field are obtained through an adapted force matching technique,[33] which refines the force field iteratively by performing classical MD simulations, with force matching referenced to first-principles quantum-mechanical calculations. A full description of the method and additional technical details are provided in the Methods section and the Supporting Information.

To cover the range of common experimental conditions, we performed the parametrization at two different temperatures, 300 and 373 K, with two different Li^+:EO ratios, 1:10 and 1:20, respectively. The optimization process is summarized in Tables 1, S1, S2, and S3. For all parametrization runs, the initial trial

Table 1. Optimization of Parameters at a Li^+:EO Ratio of 1:10 and a Temperature of 300 K[a]

iteration	1	2	3	4	5	6	7
scaling factor	1.0	0.81	0.78	0.79	0.79	0.78	0.78
$\epsilon_{Li-O(PEO)}$	0.05	0.05	0.05	0.05	0.06	0.06	0.06
$\sigma_{Li-O(PEO)}$	2.48	2.43	2.41	2.42	2.41	2.40	2.40
$\epsilon_{Li-O(TFSI^-)}$	0.06	0.07	0.07	0.07	0.07	0.07	0.07
$\sigma_{Li-O(TFSI^-)}$	2.51	2.35	2.32	2.33	2.32	2.31	2.31
obj funct (%)	23.7	13.0	10.7	10.7	10.7	10.7	10.9

[a]The objective function is defined as the mean-squared difference between force field forces and reference over the mean-squared forces, as shown in eq 1 in the Supporting Information. The units of ϵ and σ shown here are kcal/mol and Å. The optimization processes for the other Li^+:EO ratios and temperatures are shown in Tables S1−S3.

values are taken from the existing OPLS force field, where the charges on Li^+ and $TFSI^-$ are set to $+1e$ and $-1e$, respectively. To focus on nonbonded interactions, only the forces on Li^+ are matched in the force matching steps. The objective function is therefore defined as the mean-squared difference between force field forces and the reference, normalized by the mean-squared reference forces. In the first iteration, the objective function is in the range between 20% and 40% among the four different parametrization conditions. The resulting charge-scaling factor becomes ∼0.8, and the LJ radii decrease slightly for all parametrization conditions. The parameters tend to stabilize after the first iteration and converge within several iterations, with the objective functions also stabilizing at 10%−12%. The most notable result from the parametrization is that the scaling factor converges to ∼0.8 for all cases, which is consistent with the value that is commonly applied in the literature simulations. In addition, the converged LJ parameters are relatively uniform. We gathered all the reference frames and forces from the last iteration of all 4 cases and performed a combined run of force matching. This combined run yielded consistent results with each individual parametrization condition, with the scaling factor converging to 0.79 and an overall objective function of 11.1%. Therefore, we consider this final set of parameters to be generally applicable in the Li^+:EO range that was covered in the optimization process.

We carried out MD simulations with the parameters obtained above to benchmark the diffusion properties captured by this model. We performed MD simulations of Li^+−$TFSI^-$−PEO systems at Li^+:EO ratios of 1:10 and 1:18 and compared our results to available experimental reports.[34,35] As shown in Figure S1 and Table S8, simulations spanning several hundreds of nanoseconds are necessary to approach the diffusive regime for Li^+, even at elevated temperatures. The comparison between simulation and experimental diffusion coefficients is shown in Figure 2. Figure 2a shows the salt diffusion coefficient at Li^+:EO = 1:18, where the experimental value falls between the original and charge-scaled results. Note that the molecular weight of the simulated PEO has a molecular weight (MW = 1582) below the entanglement MW (MW ≈ 2000)[36−38] and is expected to lead to slightly higher diffusivities[10,38,39] than those measured for entangled polymers (MW = 600,000).[35] Figure 2b shows the Li^+ diffusion coefficients at Li^+:EO = 1:10. The simulated PEO in this case has lower MW than that used in experiments (MW = 2480)[34] and is expected to predict slightly higher diffusivities. Our results show that the diffusivities are slightly underestimated by the charge-scaled model, but they still represent a significant improvement over the original OPLS force field, by approximately one order of magnitude. Overall, the charge-scaled model provides significantly better agreement with experimental measurements than the original OPLS, consistent with existing reports.[9−19] We also calculated the diffusion coefficients with a charge-scaling factor of 0.79, but without modifying the LJ parameters of the original OPLS force field. The results are shown in Figure 2b, labeled as "scaled-only". The diffusion coefficients with and without modified LJ parameters are very similar, confirming that the diffusivity of Li^+ is dominated by electrostatic interactions.

The Li^+ transference number, which is a measure of the contribution of Li^+ diffusion to the overall ionic conductivity, is calculated here for the case 1:18, where experimental data are available. We find a decrease in the Li^+ transference number from 0.28 to 0.21 after the charge-scaling model is applied. Note that both estimates are within the range of the experimentally reported value, 0.24.[35] This decreasing trend is consistent with a previous report.[11] Since only the charges on the ions are scaled, the electrostatic stabilization between Li^+ and its anion is weakened more significantly than that between Li^+ and the polymer, thereby leading to a decreasing trend. This is also an indication that further scaling of the ion charge would lead to larger disagreements with experiment.

https://doi.org/10.1021/acsmacrolett.4c00368
ACS Macro Lett. 2024, 13, 1258−1264

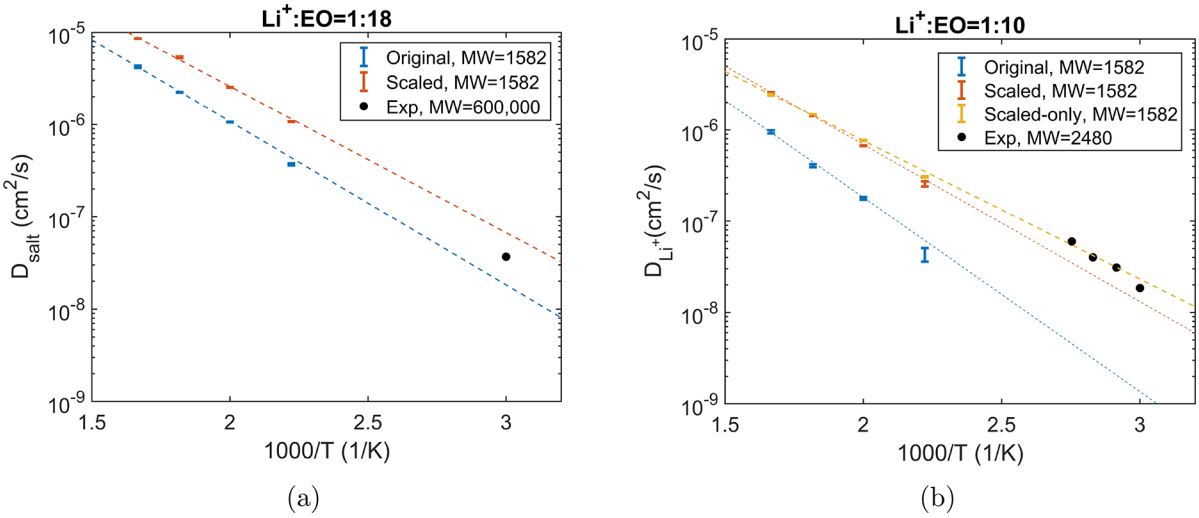

Figure 2. (a) Salt diffusion coefficient for Li^+:EO = 1:18 and (b) Li^+ diffusion coefficient for Li^+:EO = 1:10 from MD simulations, with comparisons to experimental data.[34,35] The corresponding mean-squared displacement plots are shown in Figure S1, and the convergence behaviors are shown in Table S8.

Table 2. Final Set of Parameters Developed in This Work[a]

parameter	value
scaling factor	0.79
$\epsilon_{Li-O(PEO)}$	0.06
$\sigma_{Li-O(PEO)}$	2.39
$\epsilon_{Li-O(TFSI^-)}$	0.07
$\sigma_{Li-O(TFSI^-)}$	2.31
obj funct (%)	11.1

[a]The units of ϵ and σ shown here are kcal/mol and Å.

We performed a conformational analysis of the arrangement between Li^+ and the oxygen atoms from PEO and $TFSI^-$. The radial distribution functions (RDFs) at 300 K are shown in Figure 3. At both 1:10 and 1:18 concentrations, the positions of the first coordination shells between Li^+ and PEO or $TFSI^-$ oxygens differ by less than 0.2 Å after charge scaling, which is relatively minor. Charge scaling mainly affects peak heights. After the charge scaling, Li ions coordinate stronger with PEO oxygens and weaker with $TFSI^-$ oxygens. By accumulating the coordination numbers from the integrated RDFs for the 1:10 case, we find that the Li^+−PEO oxygen coordination numbers are 3.03/4.20 for the original/charge-scaled models, and the Li^+−$TFSI^-$ oxygen coordination numbers are 2.37/1.13, summing up to 5.40/5.33 as total oxygen coordination. For the 1:18 case, the numbers are 4.53/5.32, 1.21/0.10, summing up to 5.74/5.42. In both cases, we employed a first solvation shell cutoff distance of 2.7 Å. This analysis indicates that for each Li^+, the number of oxygens it coordinates to remains approximately unchanged in the different models, but they coordinate more with the PEO oxygens in the charge-scaled model. The total oxygen coordination numbers are in line with previous neutron diffraction isotopic substitution (NDIS) experiments at 296 K, for the Li^+−$TFSI^-$−PEO system with a EO:Li ratio of 7.5:1, where a total of 4.9 oxygen atoms were observed within the first coordination shell.[40] For comparison, a previous simulation study using a many-body polarizable force field reported a total oxygen coordination number of 4.6 at an EO:Li ratio of 7.5:1 and a temperature of 395 K.[41]

The Li ions adopt three common conformational states: Li^+ aggregates (LAG), contact ion pairs (CIP), and solvent separated ion pairs (SSIP), corresponding to Li^+ that only coordinate to $TFSI^-$, coordinate with both $TFSI^-$ and PEO, and only coordinate to PEO.[9,42] The conformational representations are listed in Figure 4a−c. We analyzed the frequency of speciation for the three coordination states, and the results at 300 K are shown in Figure 4d. Unsurprisingly, Li^+s in the 1:18 case coordinate less with $TFSI^-$ compared to the 1:10 case, due to an overall lower ion concentration and less saturated PEO coordinating sites. Between the models, the charge-scaled model predicts a significant increase of the SSIP state, from 0.18 to 0.59 for the 1:10 case and 0.31 to 0.85 for the 1:18 case. While direct comparison to experiment is challenging, a recent study of Li^+ diffusion in fluoroether solvents indicated that a scaling factor of 0.8 yielded the best agreement with experimental conformational data, outperforming both cases with no scaling factor and those with different scaling factors.[9] This additional evidence suggests that the charge-scaling factor identified here enhances the predicted solvation structure in Li^+ electrolyte systems. In addition to the 300 K case, the same conformational analysis was performed at 333 K (Figure S2), and the results were consistent with those at 300 K.

To better quantify the impact of charge scaling on the thermodynamics, we calculated the averaged interaction energies between a Li^+ and the rest of the system at 300 K (Table S9). The calculations yield −201.5 ± 26.8/−206.2 ± 23.2 kcal/mol for Li^+:EO = 1:10/1:18 before scaling and −128.9 ± 17.2/−132.9 ± 12.3 with the charge-scaled parameters. Previous first-principles calculations reported 129.8[43] and 149.6[44] kcal/mol, in good agreement with the charge-scaled results. An energy decomposition suggests that the absolute values of electrostatic interaction energies decrease by ∼70−75 kcal/mol out of a total of ∼210 kcal/mol after the scaled-charge parameters are applied, while the changes in the van der Waals interaction energies represent only 0−1 kcal/mol out of a total of 6−7 kcal/mol. This result further confirms that the interaction between Li^+ and its surroundings is dominated by Coulombic interactions and demonstrates the significant impact of charge scaling on Li^+ thermodynamics.

https://doi.org/10.1021/acsmacrolett.4c00368
ACS Macro Lett. 2024, 13, 1258−1264

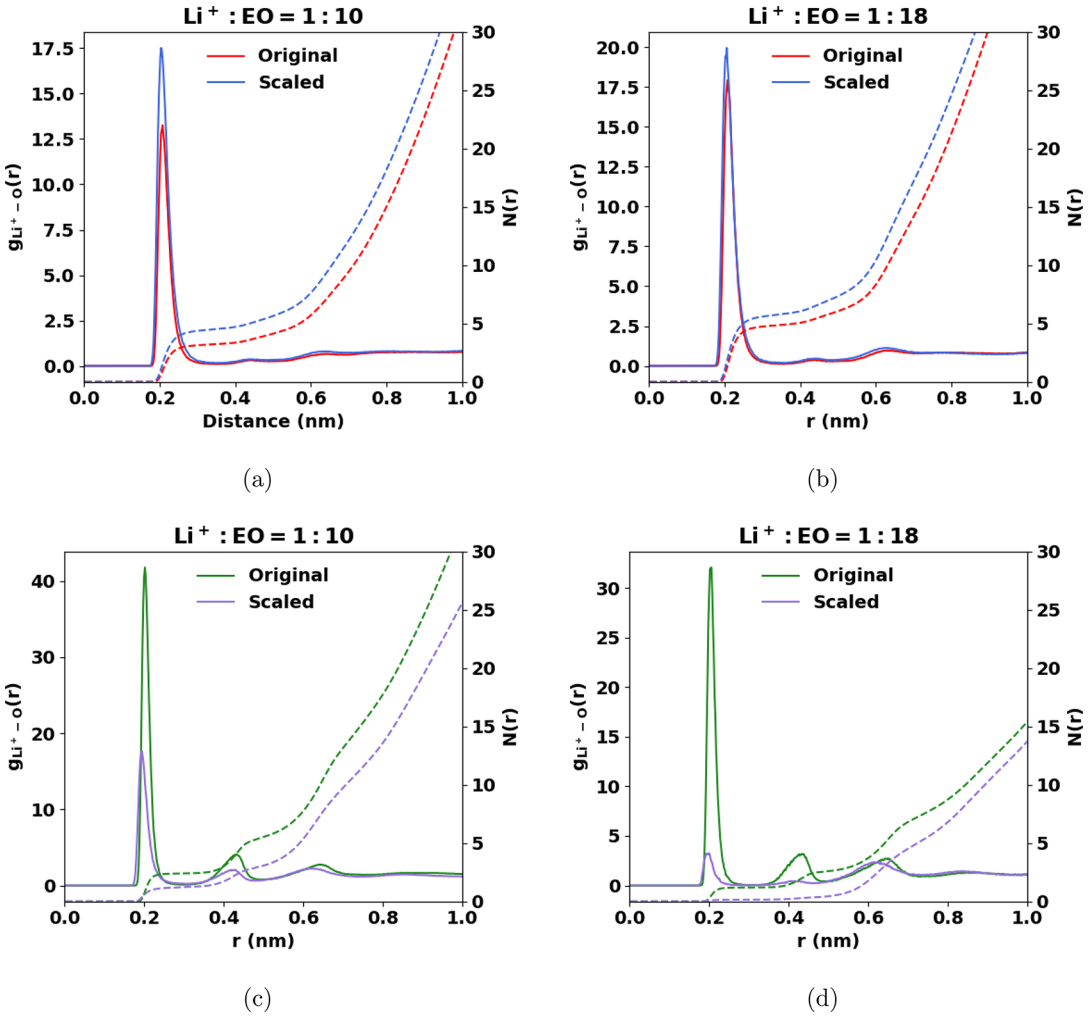

Figure 3. Radial distribution functions (RDFs) between Li^+ and PEO oxygens (a, b) and $TFSI^-$ oxygens (c, d) at Li^+:EO ratios of 1:10 (a, c) and 1:18 (b, d). The results at 333 K are shown in Figure S2.

Overall, we have reported an optimization procedure for charge scaling in force fields for Li^+ transport. Rather than empirically matching experimental data, our scaling factor is obtained through an optimized force matching to first-principles calculations, thereby providing a connection to the underlying molecular interactions. Our results suggest that a scaling factor of 0.79 is applicable for Li^+:EO ratios ranging from 1:18 to 1:10, and we provide the corresponding LJ parameters for Li−oxygen interactions. The benchmark of the force field for both diffusion and conformation provides good agreement with experiments. The force matching protocol adopted in this study is transferable to other Li^+ transport problems in the context of polymer electrolytes. The general convergence of an optimized charge-scaling factor across different conditions suggests that the charge-scaling approach provides—a useful and practical strategy to incorporate polarization effects. Compared with other more elaborate polarizable models, this approach reduces computational costs while reproducing dynamics and conformational properties in atomistic simulations of ionic transport in polymers.

METHODS

In this work, we apply a modified version of the adaptive force matching approach reported by Wang and co-workers[33] to justify the use of a scaled-charge model for Li ion in polyelectrolytes. The approach can be summarized as follows: To initiate the simulation, a set of trial parameters are introduced to perform classical MD simulations on a trial system. From the MD trajectory, frames are extracted for force calculations with hybrid quantum mechanics/molecular mechanics (QM/MM) calculations, where the atoms of interest and their surroundings are selected as the QM region. Afterwards, force matching is applied to minimize the differences between the forces calculated by the force field and the QM/MM reference, which generates a new set of trial force field parameters from an optimization process. The new parameters are then applied for a new MD run, followed by a new set of QM/MM calculations and force matching. By repeating this process iteratively, an optimized set of parameters is eventually found. This method has been successfully applied to develop accurate force fields for ion solvation in water and several other systems.[22,45,46]

In our practice, the protocol is modified to better overcome the slow relaxation of polymers. First, instead of one trial system being used for the MD simulation, we used five parallel replicas with different starting conformations. Second, an additional annealing run for each replica at 500 K was performed between iterations. Third, To accurately represent the Li^+:EO ratios, we apply full QM calculations with periodic boundary conditions, instead of QM/MM. The technical details of the MD simulations, the optimization process, and the first-principles calculations are discussed in the Supporting Information.

From MD simulations, the diffusion coefficient (D) is extracted using the Einstein relation, given by

https://doi.org/10.1021/acsmacrolett.4c00368
ACS Macro Lett. 2024, 13, 1258−1264

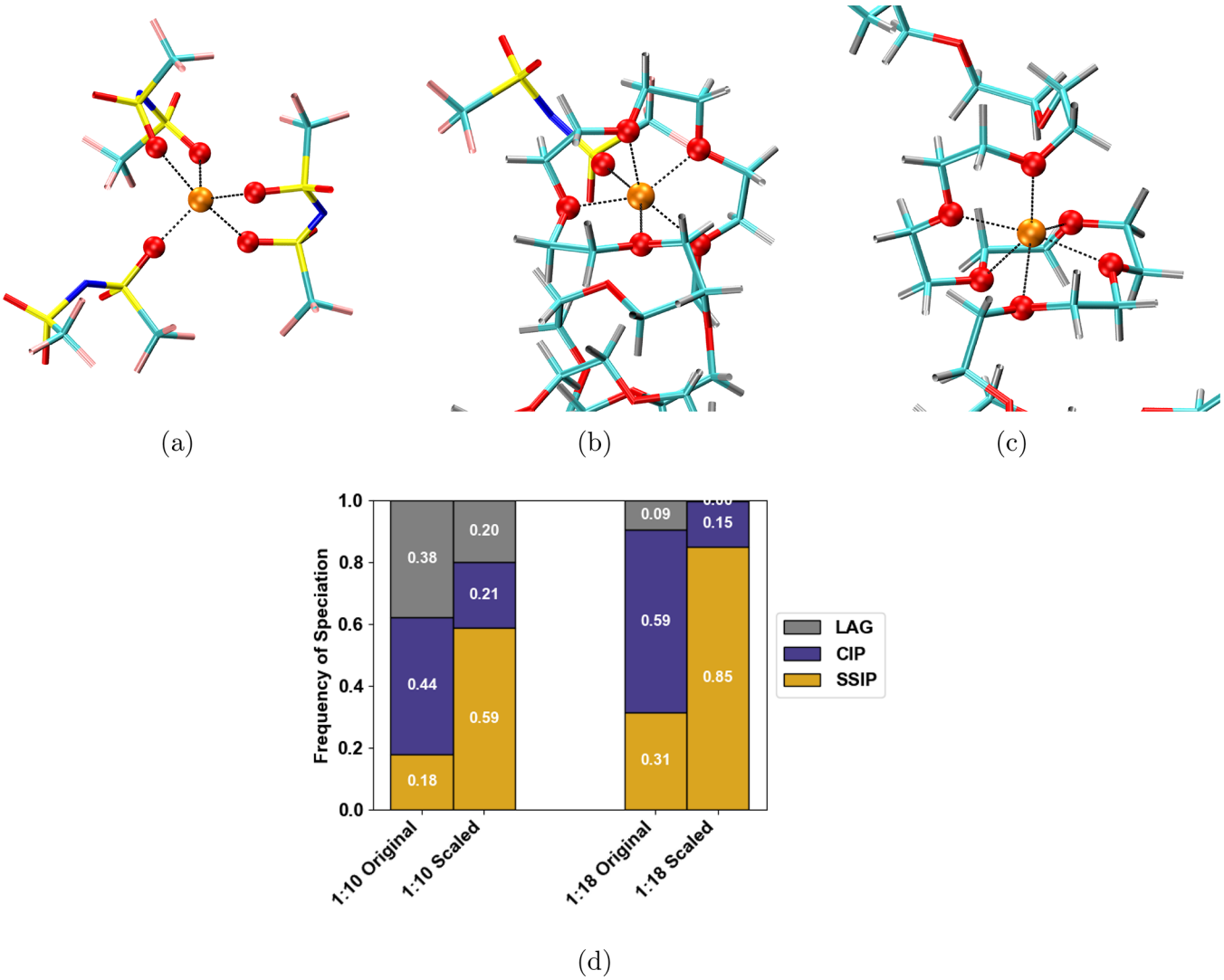

Figure 4. Snapshots of three most common conformational states (a–c) and the frequency speciation at 300 K (d) from MD simulations. The snapshots shown in (a–c) correspond to Li^+ aggregates (LAG), contact ion pairs (CIP), and solvent separated ion pairs (SSIP), corresponding to Li^+s that only coordinate to $TFSI^-$, coordinate with both $TFSI^-$ and PEO, and only coordinate to PEO. The Li^+ and coordinating oxygens are highlighted with spherical representations. For clarity, only the polymer chains or $TFSI^-$ that coordinate with Li^+ are shown in the snapshots. The color representations for the elements are Li = orange, O = red, C = cyan, N = blue, F = pink, S = yellow, and H = silver. The frequency speciation at 333 K is shown in Figure S2.

$$D = \lim_{t\to\infty}\left[\frac{1}{6t}\langle \Delta r(t)^2\rangle\right] \quad (1)$$

Here $\langle \Delta r(t)^2\rangle$ is the mean-squared displacement. In practice, we found that trajectories spanning several hundreds of nanoseconds are required to reach the diffuse regime (see Figure S1). In this work, the apparent diffusion coefficients at t = 250 ns are applied to approximate the true values. The error is estimated by the difference between t = 150 and 250 ns (Table S8). The transference number of Li^+ can be calculated from the diffusion coefficients of the ions with the following:

$$t_{Li} = \frac{D_{Li}}{D_{Li} + D_{TFSI}} \quad (2)$$

Here D_{Li} and D_{TFSI} are the diffusion coefficients of Li^+ and $TFSI^-$.

■ ASSOCIATED CONTENT

Data Availability Statement

Example inputs of the adaptive force matching applied are available at https://github.com/liangdy93/chg_scaling.git.

Supporting Information

The Supporting Information is available free of charge at https://pubs.acs.org/doi/10.1021/acsmacrolett.4c00368.

Simulation details; Figures S1–S2 and Tables S1–S9 PDF)

■ AUTHOR INFORMATION

Corresponding Author

Juan J. de Pablo – *Pritzker School of Molecular Engineering, University of Chicago, Chicago, Illinois 60637, United States;* orcid.org/0000-0002-3526-516X; Email: depablo@uchicago.edu

Authors

Dongyue Liang – *Pritzker School of Molecular Engineering, University of Chicago, Chicago, Illinois 60637, United States*

Yuxi Chen – *Pritzker School of Molecular Engineering, University of Chicago, Chicago, Illinois 60637, United States*

https://doi.org/10.1021/acsmacrolett.4c00368
ACS Macro Lett. 2024, 13, 1258–1264

Chuting Deng − *Pritzker School of Molecular Engineering, University of Chicago, Chicago, Illinois 60637, United States;* orcid.org/0000-0002-0416-178X

Complete contact information is available at: https://pubs.acs.org/10.1021/acsmacrolett.4c00368

Author Contributions

CRediT: **Dongyue Liang** data curation, formal analysis, investigation, methodology, software, visualization, writing - original draft, writing - review & editing; **Yuxi Chen** formal analysis, visualization, writing - original draft, writing - review & editing; **Chuting Deng** writing - original draft, writing - review & editing; **Juan J. de Pablo** conceptualization, funding acquisition, project administration, resources, supervision, writing - original draft, writing - review & editing.

Notes

The authors declare no competing financial interest.

■ ACKNOWLEDGMENTS

The authors are grateful to Paul Nealey for helpful discussions. This work was supported by the Department of Energy, Office of Basic Energy Sciences, Division of Materials Science and Engineering. Several of the codes and algorithms employed in this work were developed with support from the Midwest Integrated Center for Computational Materials (MICCoM). The authors gratefully acknowledge the use of the computational resources at the University of Chicago's Research Computing Center (RCC) and the use of Bebop cluster in the Laboratory Computing Resource Center at Argonne National Laboratory.

■ REFERENCES

(1) Ngai, K. S.; Ramesh, S.; Ramesh, K.; Juan, J. C. A review of polymer electrolytes: fundamental, approaches and applications. *Ionics* **2016**, *22*, 1259−1279.
(2) Hallinan, D. T., Jr.; Balsara, N. P. Polymer electrolytes. *Annu. Rev. Mater. Res.* **2013**, *43*, 503−525.
(3) Long, L.; Wang, S.; Xiao, M.; Meng, Y. Polymer electrolytes for lithium polymer batteries. *J. Mater. Chem. A* **2016**, *4*, 10038−10069.
(4) Mogurampelly, S.; Borodin, O.; Ganesan, V. Computer simulations of ion transport in polymer electrolyte membranes. *Annu. Rev. Chem. Biomol. Eng.* **2016**, *7*, 349−371.
(5) Zhang, H.; Chen, F.; Carrasco, J. Nanoscale modelling of polymer electrolytes for rechargeable batteries. *Energy Storage Mater.* **2021**, *36*, 77−90.
(6) Shah, A. A.; Luo, K.; Ralph, T.; Walsh, F. Recent trends and developments in polymer electrolyte membrane fuel cell modelling. *Electrochim. Acta* **2011**, *56*, 3731−3757.
(7) Mabuchi, T.; Nakajima, K.; Tokumasu, T. Molecular dynamics study of Ion transport in polymer electrolytes of All-solid-state Li-Ion batteries. *Micromachines* **2021**, *12*, 1012.
(8) Borodin, O.; Smith, G.; Geiculescu, O.; Creager, S. E.; Hallac, B.; DesMarteau, D. Li+ transport in lithium sulfonylimide- oligo (ethylene oxide) ionic liquids and oligo (ethylene oxide) doped with LiTFSI. *J. Phys. Chem. B* **2006**, *110*, 24266−24274.
(9) Chen, Y.; Lee, E. M.; Gil, P. S.; Ma, P.; Amanchukwu, C. V.; de Pablo, J. J. Molecular engineering of fluoroether electrolytes for lithium metal batteries. *Mol. Syst. Des. Eng.* **2023**, *8*, 195−206.
(10) Brooks, D. J.; Merinov, B. V.; Goddard III, W. A.; Kozinsky, B.; Mailoa, J. Atomistic description of ionic diffusion in PEO−LiTFSI: Effect of temperature, molecular weight, and ionic concentration. *Macromolecules* **2018**, *51*, 8987−8995.
(11) Fang, C.-E.; Tsai, Y.-C.; Scheurer, C.; Chiu, C.-C. Revised atomic charges for OPLS force field model of poly (ethylene oxide): Benchmarks and applications in polymer electrolyte. *Polymers* **2021**, *13*, 1131.
(12) Costa, L. T.; Sun, B.; Jeschull, F.; Brandell, D. Polymer-ionic liquid ternary systems for Li-battery electrolytes: Molecular dynamics studies of LiTFSI in a EMIm-TFSI and PEO blend. *J. Chem. Phys.* **2015**, *143*, 024904.
(13) Mogurampelly, S.; Ganesan, V. Structure and mechanisms underlying ion transport in ternary polymer electrolytes containing ionic liquids. *J. Chem. Phys.* **2017**, *146*, 074902.
(14) Van Zon, A.; Mos, B.; Verkerk, P.; De Leeuw, S. On the dynamics of PEO-NaI polymer electrolytes. *Electrochim. Acta* **2001**, *46*, 1717−1721.
(15) Müller-Plathe, F.; van Gunsteren, W. F. Computer simulation of a polymer electrolyte: Lithium iodide in amorphous poly (ethylene oxide). *J. Chem. Phys.* **1995**, *103*, 4745−4756.
(16) Zhang, Z.; Zofchak, E.; Krajniak, J.; Ganesan, V. Influence of polarizability on the structure, dynamic characteristics, and ion-transport mechanisms in polymeric ionic liquids. *J. Phys. Chem. B* **2022**, *126*, 2583−2592.
(17) Keith, J. R.; Mogurampelly, S.; Aldukhi, F.; Wheatle, B. K.; Ganesan, V. Influence of molecular weight on ion-transport properties of polymeric ionic liquids. *Phys. Chem. Chem. Phys.* **2017**, *19*, 29134−29145.
(18) Ebadi, M.; Eriksson, T.; Mandal, P.; Costa, L. T.; Araujo, C. M.; Mindemark, J.; Brandell, D. Restricted ion transport by plasticizing side chains in polycarbonate-based solid electrolytes. *Macromolecules* **2020**, *53*, 764−774.
(19) Deng, C.; Bennington, P.; Sánchez-Leija, R. J.; Patel, S. N.; Nealey, P. F.; de Pablo, J. J. Entropic Penalty Switches Li+ Solvation Site Formation and Transport Mechanisms in Mixed Polarity Copolymer Electrolytes. *Macromolecules* **2023**, *56*, 8069−8079.
(20) Kann, Z.; Skinner, J. A scaled-ionic-charge simulation model that reproduces enhanced and suppressed water diffusion in aqueous salt solutions. *J. Chem. Phys.* **2014**, *141*, 104507.
(21) McDaniel, J. G.; Yethiraj, A. Influence of electronic polarization on the structure of ionic liquids. *J. Phys. Chem. Lett.* **2018**, *9*, 4765−4770.
(22) Akin-Ojo, O.; Wang, F. Improving the point-charge description of hydrogen bonds by adaptive force matching. *J. Phys. Chem. B* **2009**, *113*, 1237−1240.
(23) Leontyev, I.; Stuchebrukhov, A. Electronic continuum model for molecular dynamics simulations. *J. Chem. Phys.* **2009**, *130*, 085102.
(24) Gudla, H.; Zhang, C.; Brandell, D. Effects of solvent polarity on Li-ion diffusion in polymer electrolytes: An all-atom molecular dynamics study with charge scaling. *J. Phys. Chem. B* **2020**, *124*, 8124−8131.
(25) Singh, U. C.; Kollman, P. A. An approach to computing electrostatic charges for molecules. *J. Comput. Chem.* **1984**, *5*, 129−145.
(26) Bader, R. *Atoms in Molecules: A Quantum Theory*; Oxford University Press: Oxford, UK, 1994.
(27) Huang, J.; Rauscher, S.; Nawrocki, G.; Ran, T.; Feig, M.; De Groot, B. L.; Grubmüller, H.; MacKerell, A. D., Jr. CHARMM36m: an improved force field for folded and intrinsically disordered proteins. *Nat. Methods* **2017**, *14*, 71−73.
(28) Yoo, J.; Aksimentiev, A. New tricks for old dogs: improving the accuracy of biomolecular force fields by pair-specific corrections to non-bonded interactions. *Phys. Chem. Chem. Phys.* **2018**, *20*, 8432−8449.
(29) Jorgensen, W. L.; Maxwell, D. S.; Tirado-Rives, J. Development and testing of the OPLS all-atom force field on conformational energetics and properties of organic liquids. *J. Am. Chem. Soc.* **1996**, *118*, 11225−11236.
(30) Doherty, B.; Zhong, X.; Gathiaka, S.; Li, B.; Acevedo, O. Revisiting OPLS force field parameters for ionic liquid simulations. *J. Chem. Theory Comput.* **2017**, *13*, 6131−6145.
(31) Aqvist, J. Ion-water interaction potentials derived from free energy perturbation simulations. *J. Phys. Chem.* **1990**, *94*, 8021−8024.

(32) Kohagen, M.; Lepsik, M.; Jungwirth, P. Calcium binding to calmodulin by molecular dynamics with effective polarization. *J. Phys. Chem. Lett.* **2014**, *5*, 3964−3969.
(33) Akin-Ojo, O.; Song, Y.; Wang, F. Developing ab initio quality force fields from condensed phase quantum-mechanics/molecular-mechanics calculations through the adaptive force matching method. *J. Chem. Phys.* **2008**, *129*, 064108.
(34) Hayamizu, K.; Akiba, E.; Bando, T.; Aihara, Y. ^{1}H, ^{7}Li, and ^{19}F nuclear magnetic resonance and ionic conductivity studies for liquid electrolytes composed of glymes and polyetheneglycol dimethyl ethers of $CH_3O(CH_2CH_2O)_nCH_3$ (n= 3−50) doped with $LiN(SO_2CF_3)_2$. *J. Chem. Phys.* **2002**, *117*, 5929−5939.
(35) Wang, H.; Im, D.; Lee, D.; Matsui, M.; Takeda, Y.; Yamamoto, O.; Imanishi, N. A composite polymer electrolyte protect layer between lithium and water stable ceramics for aqueous lithium-air batteries. *J. Electrochem. Soc.* **2013**, *160*, A728.
(36) De Gennes, P.-G. *Scaling Concepts in Polymer Physics*; Cornell University Press: 1979.
(37) Wool, R. P. Polymer entanglements. *Macromolecules* **1993**, *26*, 1564−1569.
(38) Gao, K. W.; Balsara, N. P. Electrochemical properties of poly (ethylene oxide) electrolytes above the entanglement threshold. *Solid State Ionics* **2021**, *364*, 115609.
(39) Timachova, K.; Watanabe, H.; Balsara, N. P. Effect of molecular weight and salt concentration on ion transport and the transference number in polymer electrolytes. *Macromolecules* **2015**, *48*, 7882−7888.
(40) Mao, G.; Saboungi, M.-L.; Price, D. L.; Armand, M. B.; Howells, W. Structure of liquid PEO-LiTFSI electrolyte. *Phys. Rev. Lett.* **2000**, *84*, 5536.
(41) Borodin, O.; Smith, G. D. Mechanism of ion transport in amorphous poly (ethylene oxide)/LiTFSI from molecular dynamics simulations. *Macromolecules* **2006**, *39*, 1620−1629.
(42) Fong, K. D.; Self, J.; Diederichsen, K. M.; Wood, B. M.; McCloskey, B. D.; Persson, K. A. Ion transport and the true transference number in nonaqueous polyelectrolyte solutions for lithium ion batteries. *ACS Cent. Sci.* **2019**, *5*, 1250−1260.
(43) Johansson, P. First principles modelling of amorphous polymer electrolytes: Li+−PEO, Li+−PEI, and Li+−PES complexes. *Polymer* **2001**, *42*, 4367−4373.
(44) Johansson, P.; Tegenfeldt, J.; Lindgren, J. Modelling amorphous lithium salt−PEO polymer electrolytes: ab initio calculations of lithium ion−tetra-, penta-and hexaglyme complexes. *Polymer* **1999**, *40*, 4399−4406.
(45) Li, J.; Wang, F. Accurate prediction of the hydration free energies of 20 salts through adaptive force matching and the proper comparison with experimental references. *J. Phys. Chem. B* **2017**, *121*, 6637−6645.
(46) Li, J.; Wang, F. Pairwise-additive force fields for selected aqueous monovalent ions from adaptive force matching. *J. Chem. Phys.* **2015**, *143*, 194505.

https://doi.org/10.1021/acsmacrolett.4c00368
ACS Macro Lett. 2024, 13, 1258−1264